# Chapter 12
# Spatial Metabolite Profiling by Matrix-Assisted Laser Desorption Ionization Mass Spectrometry Imaging

**Berin A. Boughton and Brett Hamilton**

**Abstract** Mass spectrometry imaging (MSI) is rapidly maturing as an advanced method for spatial metabolite profiling. Herein, we provide an introduction to MSI including types of instrumentation, detailed sample preparation, data collection, overview of data analysis steps, software, common standards, and new developments. Further, we provide an overview of MSI in the clinical space over the past 3 years where MSI has been deployed in diverse research areas including cancer, neurobiology, lipidomics, and metabolite profiling and mapping to name only a few. We provide several examples demonstrating the applicability of MSI to spatially profile metabolites in unique systems requiring special considerations outside of the norm.

**Keywords** Spatial metabolomics • Mass spectrometry imaging • MALDI • Matrix • High resolution

## Abbreviations

| | |
|---|---|
| 3D-MSI | Three-dimensional mass spectrometry imaging |
| 9-AA | 9-Aminoacridine |

B.A. Boughton (✉)
Metabolomics Australia, School of BioSciences, The University of Melbourne, Melbourne, VIC 3010, Australia
e-mail: baboug@unimelb.edu.au

B. Hamilton
Mater Research Institute, The University of Queensland, St Lucia, QLD, Australia

Pathology Department, Mater Health Services, South Brisbane, QLD, Australia



A. Sussulini (ed.), *Metabolomics: From Fundamentals to Clinical Applications*, Advances in Experimental Medicine and Biology,
DOI 10.1007/978-3-319-47656-8_12

| | |
|---|---|
| AP-MALDI | Atmospheric pressure matrix-assisted laser desorption ionization |
| CHCA (or HCCA) | α-Cyano-4-hydroxycinnamic acid |
| Cer | Ceramide |
| DAN | 1,5-Diaminonapthalene |
| DESI | Desorption electrospray ionization |
| DHAP | 2,5-Dihydroxyacetophenone |
| DHB | 2,5-Dihydroxybenzoic acid |
| DMAN | 1,8-Bis(dimethylamino)naphthalene |
| FA | Fatty acid |
| FFPE | Formalin-fixed paraffin embedded |
| fNPs | Functional iron nanoparticles |
| FT | Fourier transform |
| FTICR | Fourier transform ion cyclotron resonance |
| FT-IR | Fourier transform infrared spectroscopy |
| HCA | Hierarchical cluster analysis |
| Hex | Hexose |
| IR | Infrared |
| IR-MALDI | Infrared matrix-assisted laser desorption ionization |
| ITO | Indium tin oxide |
| kMSI | Kinetic mass spectrometry imaging |
| LDI | Laser desorption ionization |
| MALDI | Matrix-assisted laser desorption ionization |
| MIPC | Ceramide phosphoinositol |
| MRI | Magnetic resonance imaging |
| MS | Mass spectrometry |
| $MS^n$ | Multistage tandem mass spectrometry |
| MSI | Mass spectrometry imaging |
| MS/MS | Tandem mass spectrometry |
| *m/z* | Mass-to-charge ratio |
| NIMS | Nanostructure-initiator mass spectrometry |
| OCT | Optimal cutting temperature |
| PA | Phosphatidic acid |
| PCA | Principal component analysis |
| PC | Phosphatidylcholine |
| PE | Phosphatidylethanolamine |
| PG | Phosphatidylglycerol |
| PI | Phosphatidylinositol |
| PS | Phosphatidylserine |
| ROI | Region of interest |
| RP | Resolving power |
| SIMS | Secondary ion mass spectrometry |
| TIC | Total ion chromatogram |
| TOF | Time of flight |

## 12.1 Introduction

Recent major technical advances in mass spectrometry (MS) have increased the scope, applicability, and adoption of the technology in a vast array of research areas [1]. The number and scope of approved diagnostic clinical applications utilizing mass spectrometry are increasing and broadening extremely rapidly. In particular, the application of MS to biochemical imaging via mass spectrometry imaging (MSI) has emerged as one of the leading spatial analysis technologies for high-throughput molecular imaging in biological systems. MSI has been employed to investigate a vast range of different spatial biological questions, and there have been many excellent comprehensive reviews published in recent years [1–14]. A recent survey of MSI users has identified matrix-assisted laser desorption ionization (MALDI) as the dominant ion source (95 %), and imaging of small molecules, including drugs, metabolites, and lipids, represents approximately 80 % of the application of MSI. In this chapter, we provide an introduction to MALDI-MSI used for biological-based research.

The "omics" technologies, genomics, transcriptomics, proteomics, and metabolomics (and others), have provided insights into biochemistry, physiology, and biology and are at the forefront of discovery in modern systems biology [15]. The exquisite specialization and compartmentalization of biological systems also require spatial approaches allowing examination of "where things are happening" to unveil the full complexity of the underlying biology.

Spatial analysis can be conducted using a number of different techniques, which can be broadly categorized into two approaches: (1) in vitro isolation and extraction of individual tissue/cell types and (2) in situ, including in vivo, analysis using an imaging approach. The suite of technologies available for in situ imaging is enormously powerful and varied, including Fourier transform infrared spectroscopy, magnetic resonance imaging, electron microscopy, histochemical and immunolabeling approaches coupled to optical and fluorescence microscopy, and X-ray fluorescence microscopy, with each approach taking advantage of different physical and chemical properties of the underlying tissue to provide unique insights. MSI has a number of advantages over other imaging modalities which are directly derived from the capabilities of modern MS instrumentation, which provide molecular specificity, high sensitivity for select analytes, and the ability to measure a broad range of analytes at high mass-resolving power with high mass accuracy across wide mass ranges. Even with these advantages, it is still a challenge to provide the depth of coverage that may be achieved from alternative approaches. MSI can provide very high lateral resolutions for imaging, giving the ability to distinguish the molecular nature of fine morphological features within tissues, even down to the single-cell level. Certain MSI approaches take advantage of minimal or no sample preparation steps with a number capable of ionization directly off sample surfaces. While our spatial resolution during MALDI imaging experiments has improved in recent years, other imaging modalities can achieve higher spatial resolution, and Caprioli and coworkers have sought to integrate, or fuse if you like, these different modalities to combine the

strengths of different imaging modes for a better outcome [16]. For example, they showed that correlating modest resolution MALDI imaging (100 μm) with optical scans of H&E-stained tissue allowed the prediction of regions of interest at higher spatial resolution – the prediction at 10 μm was verified by MSI acquired at 10 μm on a serial section. This advance has the potential to combine the specificity of MALDI-MSI with optical images and other modes of imaging. The other advantage of being able to use modest resolution MALDI-MSI is that the sample throughput can be higher, as very high spatial resolution MSI on large tissue sections is not fast enough to be considered high throughput on most MALDI instruments. Recent instrumental advances have also increased the speed of which data can be collected.

MSI was first applied to biomedical imaging [17, 18] in the mid-1990s corresponding with the introduction of soft ionization techniques, in particular MALDI. MSI has significantly advanced, providing both high lateral (spatial) and high mass resolution capabilities using a variety of different ion sources and approaches. MSI has found extensive use in molecular pathology and histology where the technique is used to map the spatial distribution of proteins and small molecules including drugs, lipids, and endogenous metabolites within tissues [1, 12]. MSI has been demonstrated to have a number of advantages, including a label-free analysis and the simultaneous multiplex measurement of 100 to possibly 1000 of analytes in a single imaging experiment, providing rich high density multidimensional data. Combination of MSI with advanced software and data analysis techniques now allows the virtual microdissection and interrogation of the molecular makeup of individual tissues. Lately, advances in spatial resolution have placed MSI at the forefront of single-cell metabolomics [19, 20], demonstrating an ability to measure the metabolism of an individual specialized cell within a subpopulation of cells. The development of novel data analysis techniques is opening the doors to conducting spatial metabolomics and comparative statistics across multiple samples allowing exploration of molecular changes during disease processes and identification of biomarkers [21, 22].

## 12.2 Mass Spectrometry Imaging

There are four essential steps in a basic MSI experiment: (1) sample selection and preparation, (2) desorption and ionization, (3) mass analysis, and (4) image registration and data analysis [14]. Careful control of each is essential to enable generation of high-quality images. In particular, sample selection, storage, and preparation have a disproportionate impact on the final results; there are many potential pitfalls that must be avoided as many sample preparation steps or techniques have the potential to contaminate the tissue section with exogenous material affecting reproducibility, ionization, and image quality. Fundamentally, the MSI process involves placing a suitable tissue section into an ion source, ionizing the sample and collecting a series of position-correlated mass spectra. This series of individual mass

spectra is collected in a two-dimensional (2D) array across surface of the sample using one of a range of different ion sources and mass analyzers. The most common approach is a microprobe approach where for each spatial coordinate, a single corresponding mass spectrum is collected. The resulting mass spectra represent the intensities of ionizable molecules present as their mass-to-charge ratios (*m/z*) which are then correlated with a high-resolution optical image of the tissue or histochemical stain with each spectrum assigned as an individual pixel for image generation. When the intensity value of each respective ion is plotted as an intensity map across the 2D array, the resultant reconstructed ion image represents the spatial distribution of the corresponding molecule(s). Three-dimensional (3D) approaches are also possible where serial 2D arrays from sequential tissue sections (or depth profiling) from the one tissue sample are measured and then a 3D volume is reconstructed computationally [23–25].

### *12.2.1 Ionization and Mass Analysis*

MSI first relies on the ability to form ions that are then transferred under vacuum and measured by the mass analyzer. Currently, the dominant ion source and approach is MALDI, due to a range of commercially available instruments, which are capable of delivering high spatial and mass resolution, ease of use, and broad range of applicability to a variety of biological applications (Fig. 12.1). In practice, lateral resolutions for MALDI instruments are in the range 5–50 μm. The past 3–5 years have seen an explosion in different types of ion sources available, including atmospheric pressure MALDI (AP-MALDI) and other specialized sources for ambient ionization conditions [26]. Further, a number of popular alternative ion sources exist including SIMS, desorption electrospray ionization (DESI), nano-DESI, laser ablation electrospray ionization (LAESI), and atmospheric pressure MALDI. When undertaking MSI at very high spatial resolution, there is a significant trade-off with sensitivity, because the decreased sampling area will reduce the total number of ions available for detection. In short, MSI experiments will usually involve some kind of trade-off between spatial resolution and sensitivity; however, advanced mass analyzers and detectors are now allowing the measurement of very low numbers of ions that to some degree mitigates losses in sensitivity at high lateral resolution.

The mass analyzer is the core component of a mass spectrometer, enabling determination of mass-to-charge ratio (*m/z*) of an ion. The type of mass analyzer used and spectral resolution also have a direct impact on the ability to conduct MSI experiments (Table 12.1). The most common mass analyzers used on MSI instruments include time of flight (TOF) and Fourier transform (FT), encompassing both orbitrap and ion cyclotron resonance (FTICR) instruments. To distinguish differing metabolites in tissues, there is a clear need for accurate mass and high mass-resolving instruments and/or the use of tandem MS. Low mass resolution instruments can lead to misidentification or misinterpretation due to inability to resolve peaks of similar mass in MS scans. Ion traps have been used for imaging studies,

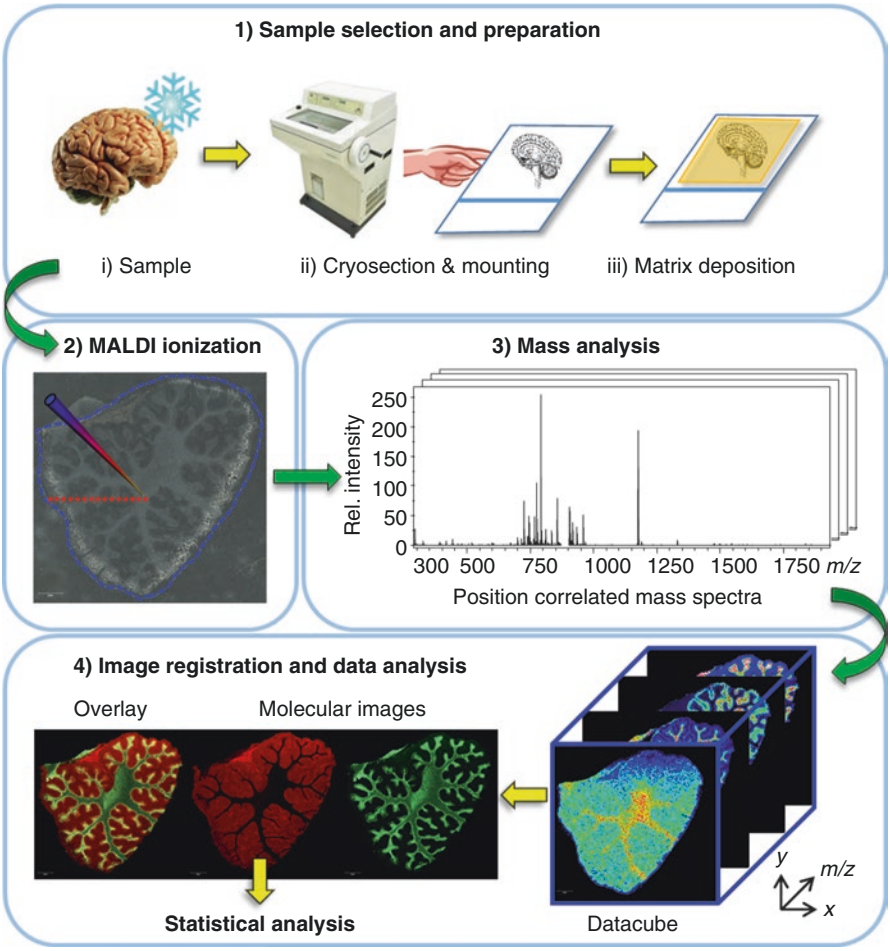


**Fig. 12.1** Matrix-assisted laser desorption ionization (MALDI) approach. (*1*) Sample selection and preparation: sample tissues are first frozen and then cryo-sectioned with resulting thin sections mounted directly to a target. A thin layer of chemical matrix is typically applied across the surface of the tissue using a spray deposition or sublimation approach; (*2*) MALDI: molecules are desorbed from the surface by preferential absorption of UV or IR light energy by the matrix, localized phase transfer generates an evolving gas plume, ions may be pre-formed in the solid phase or generated in the gas phase by ion addition or abstraction from the respective analyte; (*3*) mass analysis: individual position-correlated mass spectra are collected in a uniform array; (*4*) image registration and data analysis: spectra are combined to generate a data cube. MSI data is then defined by *x*,*y* location, *m/z*, and ion signal intensity. Individual ion images are reconstructed by plotting the ion signal intensity for a single (or multiple) *m/z* as a false color image across the 2D grid correlated with an optical image. Further statistical analysis may be conducted to identify spatial segmentation or comparative analysis across sections

**Table 12.1** List of common mass analyzers and instrument configurations detailing: mass resolution, approximate mass range, MS/MS capabilities, and acquisition speed

| Mass analyzer/ configuration | Mass resolution | Mass range (Da) | MS/MS | $MS^n$ | Acquisition speed |
|---|---|---|---|---|---|
| Ion trap | ~1000 | 50–4000 | Yes | Yes | Medium |
| TOF | 2500–40,000 | 20–500,000 | No | No | Fast |
| TOF/TOF | >20,000 | 20–500,000 | Yes | No | Fast/very fast |
| IT-TOF | 10,000 | 50–20,000 | Yes | Yes | Fast |
| IT-orbitrap | >100,000 | 40–4000 | Yes | Yes | Slow |
| FTICR | >200,000 | 10–10,000 | Yes | Yes | Slow |
| Ion mobility QTOF | 13,000/40,000 | Up to 40,000 | Yes | No | Fast |

*TOF* time of flight, *TOF/TOF* tandem TOF, *IT* ion trap, *FTICR* Fourier transform ion cyclotron resonance, *QTOF* quadrupole time of flight, *Da* dalton

and while being lower resolution mass analyzers, they do offer the possibility to perform targeted MSI experiments at $MS^2$ or $MS^n$ level, where product ions can monitored. This approach can be useful if there is sufficient signal for $MS^n$ events, and even though the MSI would be displayed for a particular product ion, whole MS and $MS^n$ spectra are acquired, meaning compound ID can be made by comparing full $MS^n$ spectra acquired during MSI analysis to spectra from standard materials. Undoubtedly, higher mass resolution is very useful in MSI experiments, where sample purification and fractionation are not possible and sample cleanup is limited, but $MS^n$ experiments using ion traps also have potential to identify compounds during MSI analysis.

The ability of a mass spectrometer to distinguish one mass peak from an ion close in mass is described by both mass resolution and resolving power (RP). MSI experiments are less sensitive than analyses that orthogonally separate analytes prior to measurement and detection; this is directly due to the extremely complex biological matrix of the tissues where vast concentration ranges of chemical entities are present with differing chemistries and molecular sizes (e.g., proteins, lipids, organic acids, amino acids, carbohydrates, inorganic ions, etc.). For MALDI experiments, the presence of high abundance low-molecular mass ions generated directly from the matrix employed can lead to significant interfering signal. Higher mass resolution allows easier identification of contributing ions and exclusion of interference from the presence of other chemical entities. Higher mass-resolving power is essential for high mass accuracy, whereby a higher RP allows identification of the center of peak and determination of the mass error, with low mass error allowing unambiguous assignment of a molecular formula aiding in identification. Modern high-resolution instruments are capable of <10 parts per million (ppm) mass error for TOF and <2 ppm mass error for FT instruments. Measurements conducted on low mass resolution instruments are typically operated in a targeted

tandem MS approach to provide molecular selectivity where specific fragment ions of single analytes are monitored, providing both molecular specificity and increased sensitivity. MSI measurements using higher resolution detectors provide the ability to unambiguously resolve a peak from the complex spectra that is generated allowing untargeted profiling-type techniques. The other exciting aspect of performing MSI with mass analyzers offering extreme resolution is that in addition to the mass accuracy measurement and the oft referred to isotope envelope, one can also measure the fine structure of each isotope peak. This fine structure is due to the very small differences in mass that exist in naturally occurring isotopes, for example, $^{34}S$ will be slightly lower in mass than $^{18}O$, and if our analyzer is capable of very high resolution, these species can be resolved and observed separately. This fine structure is characteristic of the chemical composition and can be used along with mass accuracy and traditional isotope envelope measurement to confirm molecular formulae. This approach has shown great utility in the metabolite world. For protein samples, an on-tissue digestion would be required, given the mass range of FTICR analyzers. This approach is very exciting too, because it opens the possibility of "peptide mass fingerprint"-type experiments – whereby if we confirm the presence of several peptides that emanate from an individual protein, we essentially have protein identification during an MSI analysis. This approach is important because it removes the requirement for successful $MS^2$ experiments.

A hybrid approach that uses ion mobility coupled to mass spectrometry (IM-MS) that first separates ions by their mobility in a carrier gas followed by detection by MS has recently been developed [27, 28]. IM-MS offers the ability to orthogonally separate ions in the gas phase with similar *m/z* but different shapes via collisional cross section (CCS), providing a number of benefits including better signal to noise ratio (S/N) and the potential to separate isomers according to their shape and charge [29–32]. The application of IM-MS to MALDI-MSI experiments provides much promise for the analysis of lipids, peptides, and proteins; however, the benefits of IM-MS for small molecule analysis are slowly being unveiled as higher ion mobility resolving instruments are developed.

### *12.2.2 Sample Preparation*

Prior to analysis, tissues must be collected and stored. The steps taken during both tissue collection and storage are critical for successful MSI analysis and often vary depending upon the analyte of interest. Most experiments will have a distinct timing mismatch between sample collection and analysis, requiring the storage of samples for a period of time. For most MSI analyses, tissue samples are typically flash-frozen to quench metabolism and to retain the spatial distribution of analytes and are sectioned or prepared at a later time point. Care must be taken to retain the tissue morphology during the freezing process and to preserve an accurate representation of the native tissue; soft tissues may deform and take the shape of the container

(tube or tray) within which they are frozen. Typically, to protect delicate tissues, structures, and small metabolites, a gentle freezing approach is recommended, including freezing in the atmosphere over liquid nitrogen or in cold carbon dioxide atmosphere over dry ice; alternatively, samples may be dipped into isopentane/liquid nitrogen or isopentane/dry ice slurries. Alternatively, a number of heat and microwave tissue stabilization methods have been developed for proteins and peptides [33–35].

Once samples are frozen, tissues and analytes are generally stable for months to years when stored at −80 °C. Embedding tissues within an external matrix is a common approach and is often required to ensure that suitable sections are generated from fragile tissue types that may have a tendency to fracture and crumble during sectioning. A number of different embedding media have been successfully demonstrated, including agarose [36], gelatin [20, 37–41], and aqueous carboxymethylcellulose solutions (1–5 %) [42, 43]. In general, the easier the frozen matrix is to section or the closer the properties of the matrix are to the tissue being sectioned, the easier it will be to generate suitable sections of tissue for analysis.

Standard histological workflows utilize optimal cutting temperature (OCT) compound (a solution containing ~4 % polyethylene glycols (PEG)) as an embedding medium, but this is strongly discouraged for MSI research due to absorption into the tissue and smearing of OCT across the tissue surface during cryo-sectioning, which has been shown to directly lead to ion suppression effects and loss of analyte signals [44].

While cryo-sectioning is the most commonly used method for sample preparation to access internal metabolites, there are other alternatives for tissue sectioning. Depending on the analysis method and instrument used, tissues must be prepared differently for imaging purposes, and a number of factors must be considered. External surfaces can be readily analyzed by mounting tissues directly to sample stages using double-sided tape, but for the measurement of internal distributions of metabolites, tissues must first be sectioned at an appropriate thickness to expose the underlying tissue. In particular, the type of analytes and their stability and turnover must be considered. Both the sample height and morphology may have a large effect upon the number of ions generated (due to laser focusing) and, for linear TOF instruments (LDI and MALDI), mass accuracy and resolution (due to changes in flight path length). Instruments where the detector is decoupled from the source, such as QIT, LIT, FTICR, and orbitrap instruments, are not reliant upon the sample thickness and are only limited by the physical configuration of the sample stage.

An established technique for generating thin sections from hard tissues has been recently adapted to MSI applications for delicate and difficult tissues [45]. The Kawamoto method uses an adhesive film to capture thin sections during cryo-sectioning. Once the tissue is adhered to the film, it can be transferred then fixed to a standard slide and prepared in the normal manner for MSI [46, 47].

For previously fixed tissue samples, there are a number of sample preparation protocols that have been developed for formalin-fixed paraffin-embedded (FFPE) mammalian tissue specifically for MSI analysis [48]. Previously, FFPE tissues have

been considered only suitable for examination of the distribution of metals, proteins, peptides, and other polymeric biomolecules in tissues due to the fixation extracting and degrading small molecules. More recently, the possibility of imaging small molecules from FFPE tissues has been demonstrated [49–51]. For proteins, peptides, and glycogens, further tissue preparation steps are required to retrieve antigens lengthening the sample preparation process.

Some tissue types can be very difficult to frozen section, such as secretory tissues, among other things. These tissue types benefit from a tissue fixation approach; however, FFPE fixation using formaldehyde renders the intact proteins inaccessible. This can be a problem especially for studies where transcriptome libraries do not exist – as the peptides that would be observed after antigen retrieval and enzymatic digest are meaningless in the absence of a transcriptome library. One approach for these types of sample is to utilize a fixation approach that does not involve the protein cross-linking caused by formaldehyde [52]. RCL2 and PAXgene Tissue are two products that can be used to fix tissue, which do not cross-link the proteins. Once fixed, the tissue is dehydrated (ethanol gradient) and cleared (xylene) prior to paraffin impregnation in much the same manner as routine tissue processing. This approach results in a paraffin-embedded tissue that can be sectioned very easily using a microtome. The only caveat is that the sectioned tissue cannot be floated on a water bath for mounting onto a slide, as the proteins are soluble. The carefully placed tissue section is heat mounted to a glass slide and then deparaffinized using xylene. At this stage, the tissue can have matrix applied in the same manner as any other tissue. For protein analysis, the samples are very good because the dehydration and clearing remove the lipids and other species that often reduce the sensitivity during an MSI analysis. However, the approach is clearly not ideal for analyte classes soluble in ethanol or xylene.

Once mounted to the sample carrier, the tissues are typically dehydrated under vacuum prior to either matrix deposition or direct analysis. Prior dehydration avoids any shrinkage of tissues leading to changes in sample morphology within the instrument. In MALDI-MSI using TOF detection, where a voltage is applied to the sample stage, samples are usually mounted either on glass slides coated with conductive indium tin oxide (ITO) or on reusable metal sample stages (steel or gold-coated steel). Samples are either directly freeze-thaw mounted to the surface or adhered using conductive double-sided tape [53]. Freeze-thaw mounting is generally performed by transferring the cut tissue section to the top of the sample holder (slide, plate) and then gently warming the holder from the underside using body heat. The tissue section quickly thaws and adheres to the surface of the holder. Once mounted, the sections are warmed and transferred to a vacuum desiccation chamber and dried under reduced pressure for at least 15 min before any further steps are conducted. Tissue sections may degrade rapidly and must either be stored under vacuum or, for longer periods, at −80 °C [54]. For MALDI-MSI, application of the matrix has been shown to stabilize analytes within the tissue to oxidation and degradation processes.

### 12.2.3 Tissue Washing

A commonly accepted principle of MSI analysis is to conduct the minimal amount of sample preparation steps, to avoid metabolite degradation, and to retain the distribution of analytes. However, a number of tissue washing steps can be conducted to either increase the sensitivity for certain analytes or to remove background salts to decrease salt adducts [55–57]. Mounted sections can be carefully dipped into washing solutions and then dried, before further processing such as enzymatic digestion or application of matrix. These steps have been successfully employed to increase the ionization of selected metabolites (including lipids, proteins, and peptides) in mammalian systems.

### 12.2.4 MALDI Matrix Application and In Situ Protein Digestion Strategies

MALDI relies upon an exogenous matrix, consisting typically of either small organic molecules or inorganic UV absorbent nanoparticles, which must be applied by one of a number of different techniques. Further, the achievable lateral resolution is dependent upon the size of the matrix crystals, which is in turn dependent upon the application technique employed. There are a number of approaches used to apply a MALDI matrix that can be separated into two different strategies, involving either dry deposition or wet deposition and extraction. The first, dry deposition strategy, deposits the matrix without any solvents to the top surface of a tissue section by one of two common techniques, employing handshaking of dry fine crystals of matrix onto the sample through a sieve or the use of a sublimation apparatus. A sublimation approach for deposition of matrix provides very uniform coatings with very small crystal sizes (typically in the range of 1–5 μm), allowing imaging with high spatial resolution. It is becoming one of the preferred approaches for small-molecule and lipid imaging [58].

Wet deposition strategies have also had significant attention, and there are many different techniques available for specific analyte classes. Wet deposition is one of the most common techniques for matrix deposition for MALDI-MSI analysis and is essential to conduct in situ protein digests. To conduct an in situ protein digestion, a protease, generally trypsin or α-chymotrypsin, is deposited in a buffered solution. Once uniform application of enzyme has been achieved, the sample is incubated in a humid atmosphere for a period of time, to allow localized digestion before drying and matrix application for MALDI-MSI. Matrix is first dissolved in a suitable solvent, then small droplets are applied to the surface of the tissue to be imaged, micro-extraction of endogenous molecules takes place at the solvent-tissue interface, and, as the solvent dries, analytes co-crystallize with the dissolved

matrix. The achievable lateral resolution of a wet deposition technique is predominantly dependent upon the droplet size maintained during matrix deposition. There are several different techniques reported in the literature, including homemade solutions and a range of commercially available instruments, ranging from manual airbrushing (where success is highly dependent upon the operator) to more controlled robotic spraying (HTX Imaging TM-Sprayer, HTX Technologies LLC, Carrboro, NC, USA; SunChrom SunCollect and SunCollect II plus+, SunChrom GmbH, Friedrichsdorf, Germany), automatic droplet deposition through piezoelectric vibration (ImagePrep, Bruker, Bremen, Germany), inkjet printing (ChIP 1000, Shimadzu Corp., Japan) with standard inkjet printers [59], robotic spotting (Labcyte Portrait 630 Spotter – no longer available), and automatic protein digestion robots (SunChrom SunDigest, SunCollect II plus+, SunChrom). Once deposition conditions have been optimized for specific solvents, matrix and concentration, number of passes or spray cycles, temperatures, and drying, it is possible to achieve very small crystal sizes of 5–20+ μm (in the longest dimension), allowing high-resolution imaging. A combination approach of initial dry deposition using sublimation followed by in situ "rehydration/recrystallization" by vapor exchange provides excellent results for protein and peptide imaging [7].

### *12.2.5 Matrices for MALDI Analysis*

There are a large number of matrices that are either in common use or have been recently reported in the literature for MALDI, including the main stalwarts 2,5-dihydroxybenzoic acid (DHB) [60], 2,5-dihydroxyacetophenone (DHAP) [61], sinapinic acid (SA) [62, 63], and α-cyano-4-hydroxycinnamic acid (CHCA) [64–66], which are typically used for positive-mode MALDI analysis. Recently, lithium salts of DHB, SA, CHCA, and vanillin have been demonstrated as suitable matrices for imaging hydrocarbons as the lithiated adduct [67]. 9-Aminoacridine (9-AA) [41, 68], 1,8-bis-dimethylaminonaphthalene (DMAN) [38, 69], and 1,5-diaminonaphthalene (DAN) [20, 41, 60] were reported for negative-mode analyses. 2-Aminoethyl-N-2-aminonaphthalene has also been reported as a suitable matrix [70]. Recent use of the plant metabolites quercetin and morin [71], which are structural isomers, as matrices for both positive- and negative-mode analysis, has demonstrated vastly increased detection of phospholipids in mammalian tissues when using high-resolution FTICR-MS.

More recently, DAN has been adopted for plant-based imaging, which requires very low laser energy and very small crystal size [41]. DAN has been used for MSI imaging in both positive and negative modes at very high spatial resolution (however, caution is required when using DAN as it is suspected to be a carcinogen). Further, DAN is also chemically reactive with the ability to form gas phase radicals, to induce in-source decay, and to conduct gas phase reductions of disulfide bonds [72, 73]. The use of an ambient-pressure MALDI source allows the use of volatile matrices, including liquid ion matrices and also water in the form of ice for IR-MALDI within frozen tissues [74]. Nanoparticles and colloids have been

reported as suitable matrices for MALDI-MSI, including the use of silver and gold nanoparticles for the imaging of waxes and phospholipids [75–79]. Furthermore, functional iron nanoparticles (fNPs) have been demonstrated in mammalian tissues [80]. In the case of small-molecule matrices, these can be readily removed post-MSI acquisition, washed with a suitable solvent such as ethanol or aqueous solutions, and then subjected to histochemical staining [7].

## 12.3 Data Analysis

### *12.3.1 Analytical Software and Data Analysis Techniques*

MSI experiments generate huge volumes and highly complex data; due to these properties, there is a requirement for advanced software and computational data analysis techniques to extract meaningful results from the data. Data analysis of MSI datasets was in the beginning largely limited to manual identification and mapping of individual ions but has in recent years advanced significantly and to incorporate advanced clustering and comparative visualization tools allowing spatial segmentation, identification, and comparison of multiple ions. Commercial data analysis packages include BioMap (Novartis, Basel, Switzerland), FlexImaging and ClinProTools (Bruker Daltonik, Bremen, Germany), HDI (high-definition MALDI MS imaging) coupled to MassLynx and MarkerLynx (Waters, Manchester UK), ImageQuest (Thermo Scientific, Waltham, MA, USA), MALDIVision (PREMIER Biosoft), SCiLS Lab (SCiLS Bremen, Germany), and TissueView (AB Sciex, based on BioMap). Recent adoption of the common mzML data format standard (www.imzml.org) [81] by instrument vendors and incorporation into a variety of tools or directly into the vendor software (such as FlexImaging) has allowed export of instrument-specific data into a common format, which has aided the development of vendor-independent tools for data analysis and application of advanced statistical techniques to identify underlying metabolite distributions and co-localizations. Open-source software packages include Datacube Explorer (FOM-AMOLF, Amsterdam, Netherlands) [82], Metabolite Imager (University of Texas) [83], MIRION (Justus Liebig University) [84], MSiReader (North Carolina State University) [85], OpenMSI (Lawrence Berkeley National Lab, CA, USA, http//openmsi.nersc.gov) [86], Cardinal [87], SpectViewer (www.maldi-msi.org), OmniSpect [88], MSIQuant [89], LabMSI [90], MSI.R [91], and MALDIquant [92]. Many of the current packages for MS image analysis have been developed incorporating only visualization and simple clustering techniques such as hierarchical cluster analysis (HCA) and principal component analysis (PCA).

Due to the inherent heterogeneity of MSI data, preprocessing and spectral "denoising" are recommended to obtain better results [93–95]. Preprocessing includes steps for baseline subtraction and smoothing, peak alignment and mass recalibration across the entire dataset, normalization of signal intensity, peak-picking, and data

reduction steps. A number of publications have provided detailed analysis pathways and suitable tools to examine MSI data [86, 93]. Once preprocessing steps are complete, there are three types of unsupervised approaches to identify hidden patterns and spatial distributions of metabolites: component analysis, spatial segmentation, and self-organizing maps. The first, component analysis, has been dominated by the use of principal component analysis (PCA), although other methods have been used to uncover the variation in MALDI-MSI data, including nonnegative matrix factorization, maximum autocorrelation factorization, and latent semantic analysis (see review by [93]). PCA represents the spatial patterns of molecules in terms of the set of score images, but PCA has a number of limitations including negative values (which are not present in the data) and difficulty in determining co-localized ion images for identified patterns of distribution. Spatial segmentation is a robust approach to examine MSI data where a segmentation map displays different regions in the tissues with distinct molecular composition [93]. A common approach is to use hierarchical cluster analysis (HCA), which is directly incorporated into FlexImaging. More recently, advanced spatial segmentation clustering techniques have been developed that cluster *m/z* values with distinct regions of the tissue [21, 94] and are incorporated directly into the commercial software SCiLS Lab. The third area is an emerging data analysis technique that makes use of unsupervised self-organizing maps (SOM) [96, 97] and growing self-organizing maps [98] that reduce the dimensionality of the data and allow identification of hidden patterns within the data.

Three-dimensional mass spectrometry imaging (3D-MSI) has been reported [99–101] and reviewed previously [5]. 3D-MSI is conducted using one of two approaches: (1) depth profiling on the same tissues by conducting sequential rastering events [5], which is common for SIMS [102, 103] but has also been reported for laser ablation electrospray ionization, which was used to depth profile plant leaf tissue [23], or (2) by combining multiple two-dimensional MSI measurements conducted on serial tissue sections from a single sample. Individual datasets are computationally reassembled to generate 3D volume reconstructions of individual ion distributions; for this purpose, researchers have used software such as Amira (www.fei.com), Image J (imagej.nih.gov/ij), MATLAB (www.mathworks.com), and more recently SCiLS Lab (www.scils.de) to generate 3D images.

### *12.3.2 Reporting Standards and Online Repositories*

Recent guidelines for the reporting of MSI datasets have been published [104]. The article outlines the detailed metadata and contextualizing of information that is required to fully describe an MSI dataset, and it provides eight specific reportable areas: (1) tissue samples, including the type and how the tissue was sampled; (2) tissue preparation, including methods such as washing and matrix application steps; (3) optical image, detailing information about the corresponding optical images used for MSI analysis; (4) data acquisition, detailing the instrument and parameters used to acquire the data; (5) mass spectra preprocessing, detailing the parameters used

to baseline subtract, to smooth, and to align spectra, for intensity normalization methods, for peak picking, and for data reduction methods; (6) MSI visualization, including methods for peak picking and image generation parameters; (7) compound identification, including all procedures used to identify individual metabolites; and (8) data analysis, detailing procedures, methods, and software used. Current reporting standards for identification in metabolomics experiments, including definitions for tentative, putative, and confirmed identification, have been previously published [105] and at the time of publication are currently being reviewed and updated. For MSI experiments, the ability to confirm identifications is all the more difficult due to the inability to separate isobaric compounds. Future release of reporting standards for MSI experiments in 2017 will provide detailed guidelines for MSI identification strategies. A common public repository has also recently been announced, where MSI datasets can be deposited for storage and later retrieval [106]. More recently, SCiLS Lab has announced SCiLS in the Cloud (www.scils-lab.com), an online engine capable of sharing imaging and statistical analysis results in collaborative manner. A spatial metabolomics analysis server has been released by the Alexandrov group and is available at www.alpha.metasp.eu; the OpenMSI project also offers online data analysis and sharing (http://openmsi.nersc.gov).

## 12.4 Applications

MALDI-MSI has been extensively deployed in biomedical research with several 1000 studies published since the early 1990s. A PubMed (http://www.ncbi.nlm.nih.gov/pubmed) survey of recently published literature over the years 2013 to June 2016 returns 833 publications with MALDI mass spectrometry imaging. A selection of publications from the total are referenced below along with examples of imaging lipids, peptides, and special metabolites in novel, complex, and difficult tissue types. Further, filtering to within the clinical space shows a broad range of research areas, a large number of different applications, and a dominance of the use of MALDI instruments for analysis (Fig. 12.2). A third of publications focus upon cancer ($n = 104$) with nearly another third on neurological disease ($n = 84$), reflecting this breakdown a third of analytes studies are lipids (34 %) followed by proteins and peptides (29 %) and then drugs and small molecules (24 %). The breakdown reflects that lipids derived from biological membranes are readily abundant, require few sample preparation steps, and are easily observed by MALDI-MSI.

### *12.4.1 Lipids*

Many disease models in cancer and neurobiology display significant changes in the lipid profile reflecting dramatic changes in lipid metabolism [6, 21, 107–112]. For these types of analysis, samples require relatively few preparation steps,

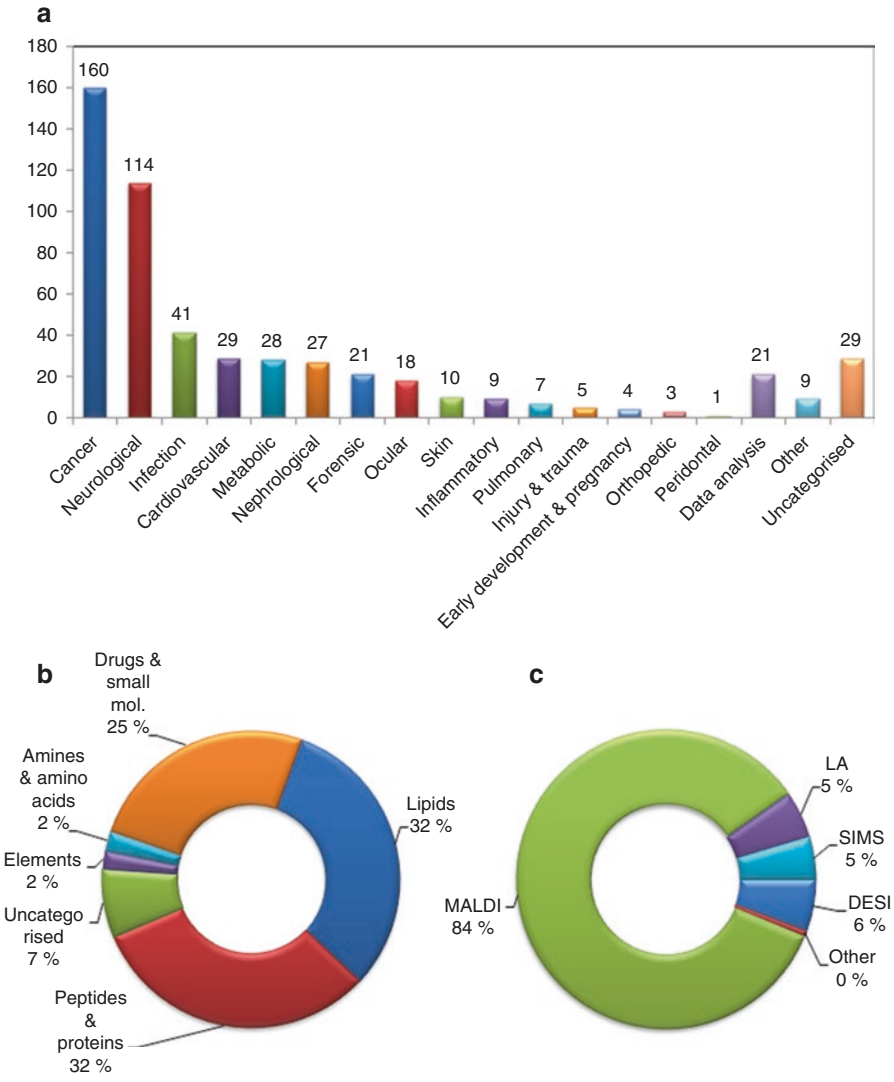


**Fig. 12.2** (**a**) Total numbers of publications by disease type and research area over 2013–2016, (**b**) Type of analyte, (**c**) Type of ionization source

cryo-sectioning of fresh frozen tissues, mounting, dehydration, and application of matrix prior to imaging. An example of the complex distribution of lipid within class and between differing classes, including fatty acids, phospholipids, ceramides, and gangliosides in kangaroo cerebellum, is shown in Fig. 12.3. Analysis in negative ionization mode is capable of tentatively identifying up to 236 different lipids and metabolites. Lipids and metabolites were identified by using the Metaspace metabolite annotation engine (www.alpha.metasp.eu) using an accepted FDR of

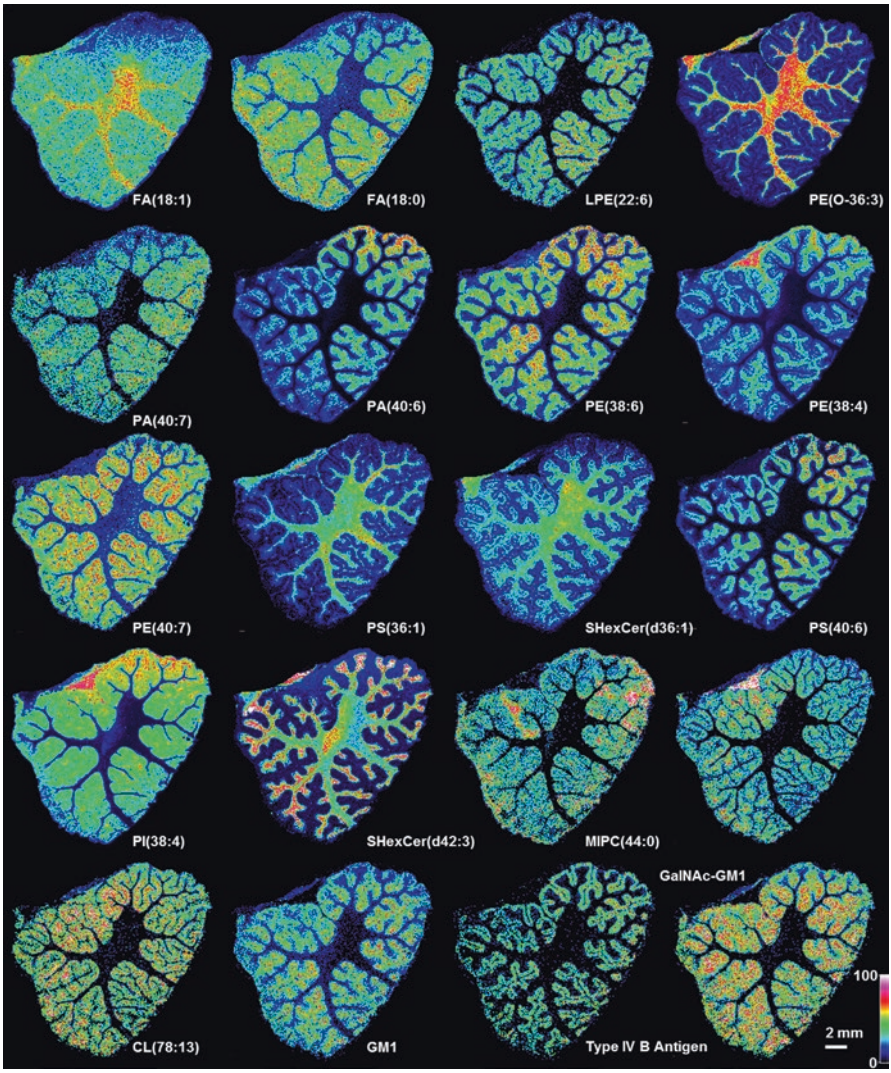


**Fig. 12.3** Distribution of different lipid classes in kangaroo cerebellum. Lipids and metabolites were identified by using the Metaspace metabolite annotation engine (www.alpha.metasp.eu) using an accepted FDR of <0.2<0.1 and an accepted mass error of <5 ppm. Sagittal section of kangaroo brain cerebellum, 20 µm thick section, thaw mounted to glass slide with 1,8-bis (pyrrolidinyl) naphthalene matrix (5 mg $mL^{-1}$ in acetone) applied by spray deposition using a HTX TM-Sprayer (8 passes, 150 µL $min^{-1}$ flow rate, 2 mm track spacing with 1 mm offset for repeat passes and 90° offset for alternate passes). Data generated on a 7 T Bruker SolariX XR MALDI-FTICR-MS in negative ionization mode, 150×150 µm spot array, 150,000 mass resolution at 400 *m/z*. Images were generated in Compass flexImaging 4.1 employing TIC normalization and scaled from 0 to 100 % of maximum ion intensity for respective ions.

<0.1. There are distinct differences in the distribution of two of the most common and simple fatty acids FA (18:0) vs. FA (18:1), differing only by a single unsaturation. The unsaturated FA (18:1) is found in high amounts within the white matter and distributed throughout the gray matter vs. the fully saturated species FA (18:0) having a preferential distribution to the gray matter. Differences in the distribution of phospholipids, PA, PE, PI, PS, and cardiolipins, ceramides including sulfated species, MIPC, and various gangliosides are observed; in particular, the simpler sulfated hexose ceramides (SHexCer (d36:1), SHexCer (d42:3)) are found in the axon-rich white matter versus the more complex MIPC and ganglioside species (GM1, Type IV Antigen, GalNAc-GM1) found in the gray matter where the majority of the neuronal cell bodies are found.

### *12.4.2 Proteins and Peptides*

Proteins, the biochemical engines of cells, and endogenous peptides including tachykinins, secretins, opioids, pancreatic peptides, and a range of other biochemically active peptides are the next most popular area of research in MSI [113–122]. Proteins can be imaged whole (but images tend to be dominated by the most abundant proteins), or for greater coverage, proteins are generally digested in situ to generate a series of peptides. A variety of different animal species produce venoms, which are cocktails of specialized peptide toxins, evolved for the capture of prey or defense against predators. Research into toxic venoms has developed into a significant area of study, in particular in the development of antivenoms and as a potential source of novel chemotherapeutics. More recently, spatial approaches have been applied to examine in vivo localization in the venom gland to better understand evolution of the toxic peptides and packaging for deployment. Within an organism venoms are generally generated in very delicate secretory tissues (glands) requiring highly specialized sample preparation methodology to preserve the structure and distribution of endogenous molecules. A recent study investigated the nature of the venoms present in the gland from a centipede, *Thereuopoda longicornis* (Fig. 12.4) [123]. Further, the study looked to determine whether compartmentalization in the gland existed. A venom gland was fixed using RCL2, dehydrated through an ethanol gradient, cleared with xylene, and impregnated with paraffin. The section was then deparaffinized using xylene prior to matrix application using an ImagePrep system (Bruker). Results demonstrated a heterogeneous distribution of differing venom peptides with the venom glands, providing insights into the evolution of venoms across centipede orders.

### *12.4.3 Endogenous Metabolites, Drugs, and Small Molecules*

Imaging of endogenous metabolites and development of spatial metabolomics techniques and tools are a rapidly expanding area [124–126]. Special or highly specific metabolites from different species, labeled drugs, or compounds are

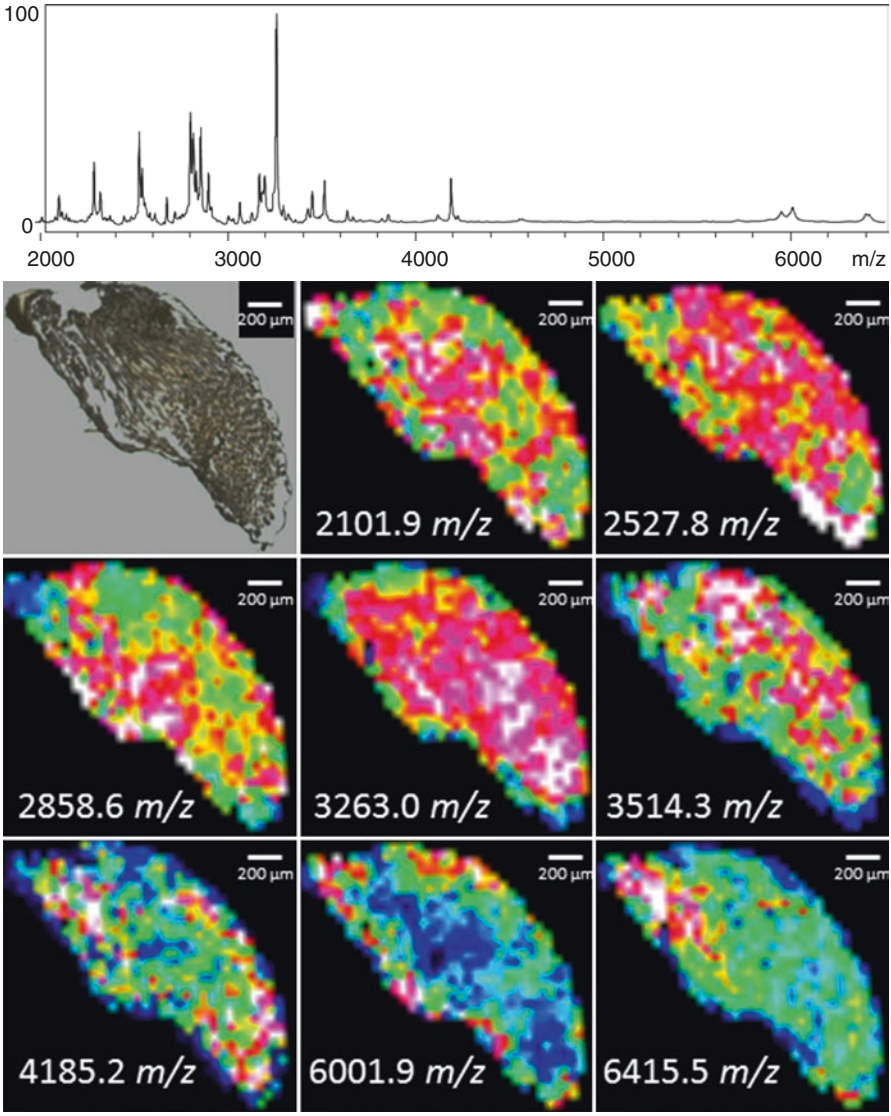


**Fig. 12.4** MALDI-MSI experiment performed in linear positive mode at 50 µm resolution using CHCA as matrix. The sample is the venom gland from a centipede, *Thereuopoda longicornis*, which was fixed using RCL2, dehydrated through an ethanol gradient, cleared with xylene, and impregnated with paraffin. Section was deparaffinized using xylene prior to matrix application using an ImagePrep system (Bruker). The aim of the study was to investigate the nature of the venom present in the gland and to determine whether compartmentalization exists (Further details can be found in Undheim et al. [123], Reprinted by permission from PNAS 2015, Copyright © 2015)

attractive targets for small-molecule MSI [124, 127–139]. These types of compounds may be readily imaged by taking advantage of their specific chemical properties and use of high mass accuracy capabilities of MS. An example is brominated alkaloid analytes from marine sponge samples [140]. The brominated species were easy to observe due to the characteristic isotope pattern that bromine confers to organic molecules. Further, the sponge sample presented many difficulties to prepare for sectioning, as the brominated alkaloids were very soluble in organic solvents, making typical fixation approaches impossible. Sectioning was ultimately achieved by embedding in OCT, prior to frozen sectioning. Pieces of the frozen sponge were dropped into the OCT; thawed sponge sample allowed too much diffusion of OCT into the sample. The sections were washed in multiple rinses of water to remove as much OCT as possible due to the deleterious impact of OCT on collecting MS. Prepared sections had CHCA matrix applied using ImagePrep (Bruker). Figure 12.5 shows the average mass spectrum observed across the tissue along the distribution of two brominated analytes at *m/z* 619 and 574 – the third figure overlays these two compounds (619, blue; 574, green) to highlight the difference in their location across the tissue.

## 12.5 Future Directions

Kinetic mass spectrometric imaging (kMSI) has recently been developed as a new analytical approach to examine combined spatiotemporally resolved metabolism. A single MSI experiment provides only a static snapshot of the underlying molecular distribution of any metabolite. By incorporation of stable isotope labeling, metabolic flux within an organism can be examined and has been demonstrated for the turnover of and biosynthesis of lipids in a tumor model (Fig. 12.6) [141]. Multimodal imaging is an emerging theme, which involves combing two or more imaging modalities to provide deeper insights into biology. A simple form of multimodal imaging is already adopted in many MSI workflows which involves generating a histochemical stained section of tissue, either a serial section or in some cases the same piece of tissue on which an MSI measurement has been conducted and then co-registering a high-resolution optical images with the acquired MSI data. This approach provides more in-depth information (tissue/cell-type distribution) and can aid in sample interpretation. The combination of MALDI and SIMS has been used extensively in plant and animal MSI imaging [142–145], where the former has been used to generate lower resolution images across a wide area and SIMS used for very high-resolution imaging of a smaller subsection of the tissue. High-resolution magnetic resonance spectroscopic imaging (MRSI) has also been combined with MSI to examine choline metabolites and cations in tumor cells [146]. More recently, the hybrid predictive technique called image fusion has been reported and combines high spatial resolution but low chemical specificity information, such as images generated from optical microscopy at high magnification, coupled to lower spatial resolution but high chemical specificity

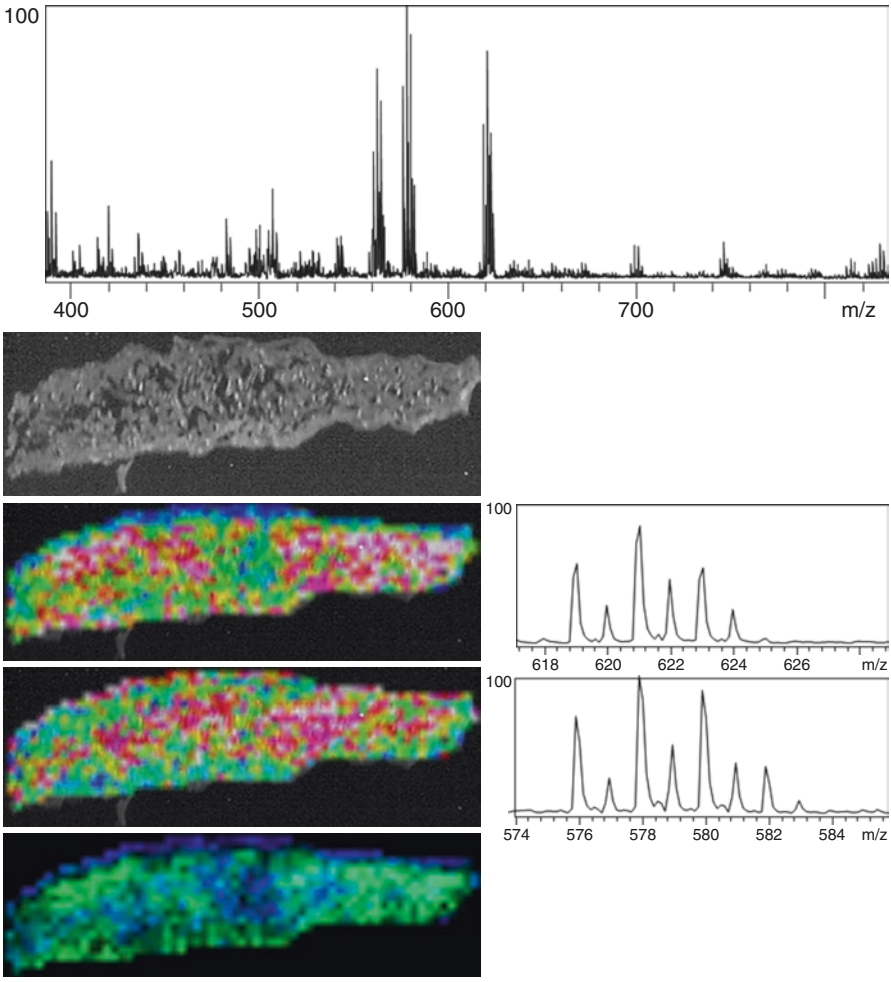


**Fig. 12.5** MALDI-MSI of marine sponge, *Stylissa flabella*, at 200 μm spatial resolution over a mass range of 200–1100 *m/z* using CHCA as a matrix. The sponge sample presented many difficulties to prepare for sectioning; the analytes of interest, brominated alkaloids, were very soluble in organic solvents, making fixation approaches impossible. Sectioning was ultimately achieved by embedding in OCT, prior to frozen sectioning. Pieces of the frozen sponge were dropped into the OCT; thawed sponge sample allowed too much diffusion of OCT into the sample. The sections were washed in multiple rinses of water to remove as much OCT as possible. Prepared sections had CHCA matrix applied using ImagePrep (Bruker). Brominated analytes were easy to observe due to the characteristic isotope pattern that bromine confers to molecules. The figure above shows the average mass spectrum observed across the tissue along the distribution of two brominated analytes at *m/z* 619 and 574 – the third figure overlays these two compounds (619, blue; 574, green) to highlight the difference in their location across the tissue (Further information can be obtained in the following references – Yarnold et al. [140] (Reprinted with permission from Molecular Biosystems, Copyright © 2012)

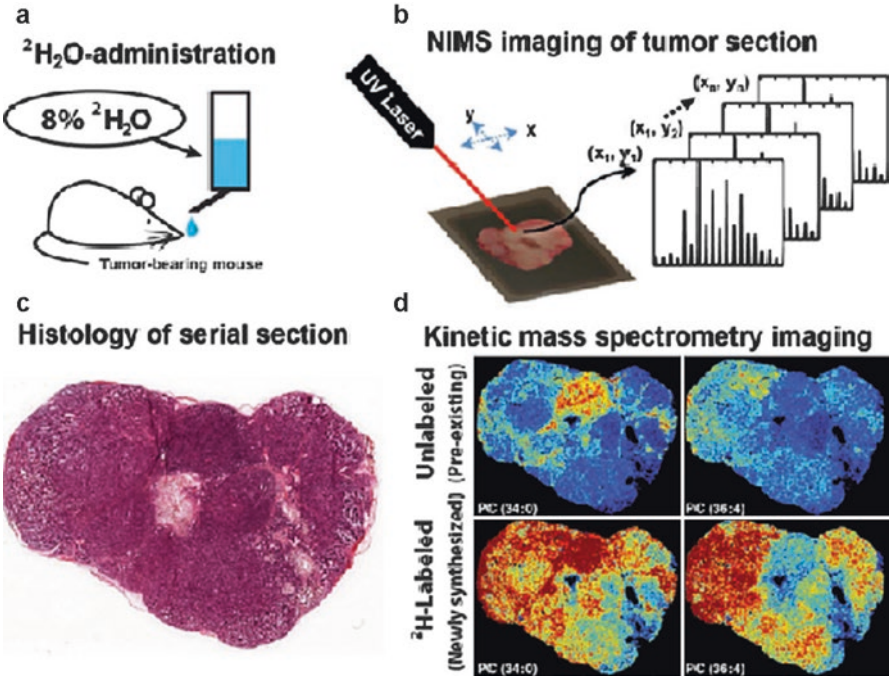


**Fig. 12.6** Example of kinetic mass spectrometric imaging – experimental workflow for using kMSI to define spatial heterogeneity of lipid composition and biosynthesis. (**a**) A tumor-bearing mouse is administered $^2H_2O$-enriched water to incorporate deuterium into tissue as a result of active metabolism. (**b**) The deuterium-enriched tumor is excised, sectioned, and imaged using NIMS. An individual mass spectrum is generated for each pixel every 50 μm, with spectra comprised of isotopologues from both $^2$H-labeled and unlabeled lipid molecules. (**c**) Serial sections of the tumor are used for histopathology correlation with kMSI results. (**d**) Deconvolution of spectra is performed to separate $^2$H-labeled and unlabeled lipids. Intensity images are generated to show the spatial distribution for both newly synthesized and preexisting lipids (Reprinted by permission from Macmillan Publishers Ltd: Scientific Reports, 3:1656 [141]. Copyright © 2013)

information, such as MSI data, to computationally predict the distribution of chemicals in the tissue sections [16]. New instrumentation is constantly being developed and recent developments include the Bruker RapiFlex TOF/TOF capable of high speed imaging (up to 80 pixels per second). Data generated from this instrument is being combined with ultrahigh mass resolution FTICR-MS imaging (relatively slow imaging) to take advantage of the benefits of each instrument to collect data quickly and provide molecular specificity [122]. Ion sources are being developed, including the MALDI-2-MS source, which incorporates a second post-ionization UV laser to generate gas phase photoionization of metabolites within the gas plume [147]. Data analysis remains a bottleneck; however, emerging MSI data analysis techniques that enable analysis of ultra-high-resolution MSI data and incorporate spatial segmentation will enhance discovery of spatially resolved metabolism. Further, development of unsupervised techniques that

utilize the spatial information within an MSI dataset and statistical techniques to discover co-occurring metabolites and significant differences in regions of tissue will unlock the power of MSI analysis speeding discovery processes.

## 12.6 Conclusion

MALDI-MSI has demonstrated application in a vast range of spatial biochemical and metabolomics research; the application of ultra-high-resolution and high mass accuracy MS provides the ability to distinguish molecular species very close in mass and accurately identifies molecular formula. High lateral resolution imaging is providing unique spatial insight into the distribution and function of many different analyte classes, and the rich, multidimensional, highly dense data is currently providing unique insights into the vast chemical complexity and specialization found within biological systems that is not possible using other methods. Challenges still exist including the development of technical methodology to examine specific classes of metabolites and advanced computational analysis to examine the data produced.

**Acknowledgments** Mr Dinaiz Thinagaran, University of Melbourne, for literature search and collation of references. Ms Sydney Currier, University of Toronto, for sample preparation of kangaroo brain images. Mr Sean O'Callaghan, Metabolomics Australia, for bioinformatics support. Metabolomics Australia, a NCRIS initiative under Bioplatforms Australia Pty Ltd. Dr Eivind Undheim, University of Queensland for *Thereuopoda longicornis* venom gland sample. Dr Anthony Carroll, Griffith University, for the *Stylissa flabellata* sample.

## References

1. Spengler B. Mass spectrometry imaging of biomolecular information. Anal Chem. 2015;87(1):64–82.
2. Chaurand P. Imaging mass spectrometry of thin tissue sections: a decade of collective efforts. J Proteomics. 2012;75(16):4883–92.
3. Jungmann JH, Heeren RM. Emerging technologies in mass spectrometry imaging. J Proteomics. 2012;75(16):5077–92.
4. Miura D, Fujimura Y, Wariishi H. In situ metabolomic mass spectrometry imaging: recent advances and difficulties. J Proteomics. 2012;75(16):5052–60.
5. Seeley EH, Caprioli RM. 3D imaging by mass spectrometry: a new frontier. Anal Chem. 2012;84(5):2105–10.
6. Gode D, Volmer DA. Lipid imaging by mass spectrometry – a review. Analyst. 2013;138(5):1289–315.
7. Norris JL, Caprioli RM. Analysis of tissue specimens by matrix-assisted laser desorption/ionization imaging mass spectrometry in biological and clinical research. Chem Rev. 2013;113(4):2309–42.
8. Rompp A, Spengler B. Mass spectrometry imaging with high resolution in mass and space. Histochem Cell Biol. 2013;139(6):759–83.

9. Wu C, Dill AL, Eberlin LS, Cooks RG, Ifa DR. Mass spectrometry imaging under ambient conditions. Mass Spectrom Rev. 2013;32(3):218–43.
10. Shariatgorji M, Svenningsson P, Andren PE. Mass spectrometry imaging, an emerging technology in neuropsychopharmacology. Neuropsychopharmacology. 2014;39(1):34–49.
11. Addie RD, Balluff B, Bovee JV, Morreau H, McDonnell LA. Current state and future challenges of mass spectrometry imaging for clinical research. Anal Chem. 2015;87(13):6426–33.
12. Aichler M, Walch A. MALDI imaging mass spectrometry: current frontiers and perspectives in pathology research and practice. Lab Invest. 2015;95(4):422–31.
13. Chughtai K, Heeren RM. Mass spectrometric imaging for biomedical tissue analysis. Chem Rev. 2010;110(5):3237–77.
14. Boughton BA, Thinagaran D, Sarabia D, Bacic A, Roessner U. Mass spectrometry imaging for plant biology: a review. Phytochem Rev. 2016;15(3):445–88.
15. Sumner LW, Lei Z, Nikolau BJ, Saito K. Modern plant metabolomics: advanced natural product gene discoveries, improved technologies, and future prospects. Nat Prod Rep. 2015;32(2):212–29.
16. Van de Plas R, Yang J, Spraggins J, Caprioli RM. Image fusion of mass spectrometry and microscopy: a multimodality paradigm for molecular tissue mapping. Nat Methods. 2015;12(4):366–72.
17. Spengler B, Kaufmann R. "Development of a new scanning UV-laser microprobe for Ion imaging and confocal microscopy", proceedings of the 42nd ASMS conference on mass spectrometry and allied topics: May 29-june 3, 1994. Chicago: ASMS; 1994.
18. Caprioli RM, Farmer TB, Gile J. Molecular imaging of biological samples: localization of peptides and proteins using MALDI-TOF MS. Anal Chem. 1997;69(23):4751–60.
19. Thiery-Lavenant G, Zavalin AI, Caprioli RM. Targeted multiplex imaging mass spectrometry in transmission geometry for subcellular spatial resolution. J Am Soc Mass Spectrom. 2013;24(4):609–14.
20. Korte AR, Yandeau-Nelson MD, Nikolau BJ, Lee YJ. Subcellular-level resolution MALDI-MS imaging of maize leaf metabolites by MALDI-linear ion trap-Orbitrap mass spectrometer. Anal Bioanal Chem. 2015;407(8):2301–9.
21. Krasny L, Hoffmann F, Ernst G, Trede D, Alexandrov T, Havlicek V, et al. Spatial segmentation of MALDI FT-ICR MSI data: a powerful tool to explore the head and neck tumor in situ lipidome. J Am Soc Mass Spectrom. 2015;26(1):36–43.
22. Steurer S, Borkowski C, Odinga S, Buchholz M, Koop C, Huland H, et al. MALDI mass spectrometric imaging based identification of clinically relevant signals in prostate cancer using large-scale tissue microarrays. Int J Cancer. 2013;133(4):920–8.
23. Nemes P, Barton AA, Vertes A. Three-dimensional imaging of metabolites in tissues under ambient conditions by laser ablation electrospray ionization mass spectrometry. Anal Chem. 2009;81(16):6668–75.
24. Ye H, Greer T, Li L. From pixel to voxel: a deeper view of biological tissue by 3D mass spectral imaging. Bioanalysis. 2011;3(3):313–32.
25. Lanekoff I, Burnum-Johnson K, Thomas M, Cha J, Dey SK, Yang P, et al. Three-dimensional imaging of lipids and metabolites in tissues by nanospray desorption electrospray ionization mass spectrometry. Anal Bioanal Chem. 2015;407(8):2063–71.
26. Monge ME, Harris GA, Dwivedi P, Fernandez FM. Mass spectrometry: recent advances in direct open air surface sampling/ionization. Chem Rev. 2013;113(4):2269–308.
27. Stauber J, MacAleese L, Franck J, Claude E, Snel M, Kaletas BK, et al. On-tissue protein identification and imaging by MALDI-ion mobility mass spectrometry. J Am Soc Mass Spectrom. 2010;21(3):338–47.
28. Jackson SN, Barbacci D, Egan T, Lewis EK, Schultz JA, Woods AS. MALDI-ion mobility mass spectrometry of lipids in negative ion mode. Anal Methods. 2014;6(14):5001–7.
29. Uetrecht C, Rose RJ, van Duijn E, Lorenzen K, Heck AJR. Ion mobility mass spectrometry of proteins and protein assemblies. Chem Soc Rev. 2010;39(5):1633–55.
30. Liu FC, Kirk SR, Bleiholder C. On the structural denaturation of biological analytes in trapped ion mobility spectrometry ─ mass spectrometry. Analyst. 2016;141(12):3722–30.

31. Kyle JE, Zhang X, Weitz KK, Monroe ME, Ibrahim YM, Moore RJ, et al. Uncovering biologically significant lipid isomers with liquid chromatography, ion mobility spectrometry and mass spectrometry. Analyst. 2016;141(5):1649–59.
32. Groessl M, Graf S, Knochenmuss R. High resolution ion mobility-mass spectrometry for separation and identification of isomeric lipids. Analyst. 2015;140(20):6904–11.
33. Goodwin RJ, Dungworth JC, Cobb SR, Pitt AR. Time-dependent evolution of tissue markers by MALDI-MS imaging. Proteomics. 2008;8(18):3801–8.
34. Goodwin RJ, Lang AM, Allingham H, Boren M, Pitt AR. Stopping the clock on proteomic degradation by heat treatment at the point of tissue excision. Proteomics. 2010;10(9):1751–61.
35. Goodwin RJ, Iverson SL, Andren PE. The significance of ambient-temperature on pharmaceutical and endogenous compound abundance and distribution in tissues sections when analyzed by matrix-assisted laser desorption/ionization mass spectrometry imaging. Rapid Commun Mass Spectrom. 2012;26(5):494–8.
36. Marques JV, Dalisay DS, Yang H, Lee C, Davin LB, Lewis NG. A multi-omics strategy resolves the elusive nature of alkaloids in Podophyllum species. Mol Biosyst. 2014;10(11):2838–49.
37. Horn PJ, Silva JE, Anderson D, Fuchs J, Borisjuk L, Nazarenus TJ, et al. Imaging heterogeneity of membrane and storage lipids in transgenic Camelina sativa seeds with altered fatty acid profiles. Plant J. 2013;76(1):138–50.
38. Ye H, Gemperline E, Venkateshwaran M, Chen R, Delaux PM, Howes-Podoll M, et al. MALDI mass spectrometry-assisted molecular imaging of metabolites during nitrogen fixation in the Medicago truncatula-Sinorhizobium meliloti symbiosis. Plant J. 2013;75(1):130–45.
39. Gemperline E, Li L. MALDI-mass spectrometric imaging for the investigation of metabolites in Medicago truncatula root nodules. J Vis Exp. 2014(85). doi:10.3791/51434.
40. Horn PJ, Sturtevant D, Chapman KD. Modified oleic cottonseeds show altered content, composition and tissue-specific distribution of triacylglycerol molecular species. Biochimie. 2014;96:28–36.
41. Korte AR, Lee YJ. MALDI-MS analysis and imaging of small molecule metabolites with 1,5-diaminonaphthalene (DAN). J Mass Spectrom. 2014;49(8):737–41.
42. Bencivenni M, Faccini A, Zecchi R, Boscaro F, Moneti G, Dossena A, et al. Electrospray MS and MALDI imaging show that non-specific lipid-transfer proteins (LTPs) in tomato are present as several isoforms and are concentrated in seeds. J Mass Spectrom. 2014;49(12):1264–71.
43. Yoshimura Y, Zaima N, Moriyama T, Kawamura Y. Different localization patterns of anthocyanin species in the pericarp of black rice revealed by imaging mass spectrometry. PLoS One. 2012;7(2):e31285.
44. Schwartz SA, Reyzer ML, Caprioli RM. Direct tissue analysis using matrix-assisted laser desorption/ionization mass spectrometry: practical aspects of sample preparation. J Mass Spectrom. 2003;38(7):699–708.
45. Gorzolka K, Kölling J, Nattkemper TW, Niehaus K. Spatio-temporal metabolite profiling of the barley germination process by MALDI MS imaging. PLoS One. 2016;11(3):e0150208.
46. Kawamoto T, Kawamoto K. Preparation of thin frozen sections from nonfixed and undecalcified hard tissues using Kawamot's film method (2012). In: Hilton JM, editor. Skeletal development and repair: methods and protocols. Totowa: Humana Press; 2014. p. 149–64.
47. Kawamoto T. Use of a new adhesive film for the preparation of multi-purpose fresh-frozen sections from hard tissues, whole-animals, insects and plants. Arch Histol Cytol. 2003;66(2):123–43.
48. Powers TW, Neely BA, Shao Y, Tang H, Troyer DA, Mehta AS, et al. MALDI imaging mass spectrometry profiling of N-glycans in formalin-fixed paraffin embedded clinical tissue blocks and tissue microarrays. PLoS One. 2014;9(9), e106255.
49. Ly A, Buck A, Balluff B, Sun N, Gorzolka K, Feuchtinger A, et al. High-mass-resolution MALDI mass spectrometry imaging of metabolites from formalin-fixed paraffin-embedded tissue. Nat Protoc. 2016;11(8):1428–43.

50. Buck A, Balluff B, Voss A, Langer R, Zitzelsberger H, Aichler M, et al. How suitable is matrix-assisted laser desorption/ionization-time-of-flight for metabolite imaging from clinical formalin-fixed and paraffin-embedded tissue samples in comparison to matrix-assisted laser desorption/ionization-Fourier transform ion cyclotron resonance mass spectrometry? Anal Chem. 2016;88(10):5281–9.
51. Buck A, Ly A, Balluff B, Sun N, Gorzolka K, Feuchtinger A, et al. High-resolution MALDI-FT-ICR MS imaging for the analysis of metabolites from formalin-fixed, paraffin-embedded clinical tissue samples. J Pathol. 2015;237(1):123–32.
52. Undheim EAB, Sunagar K, Hamilton BR, Jones A, Venter DJ, Fry BG, et al. Multifunctional warheads: diversification of the toxin arsenal of centipedes via novel multidomain transcripts. J Proteomics. 2014;102:1–10.
53. Burrell M, Earnshaw C, Clench M. Imaging matrix assisted laser desorption ionization mass spectrometry: a technique to map plant metabolites within tissues at high spatial resolution. J Exp Bot. 2007;58(4):757–63.
54. Patterson NH, Thomas A, Chaurand P. Monitoring time-dependent degradation of phospholipids in sectioned tissues by MALDI imaging mass spectrometry. J Mass Spectrom. 2014;49(7):622–7.
55. Seeley EH, Oppenheimer SR, Mi D, Chaurand P, Caprioli RM. Enhancement of protein sensitivity for MALDI imaging mass spectrometry after chemical treatment of tissue sections. J Am Soc Mass Spectrom. 2008;19(8):1069–77.
56. van Hove ER, Smith DF, Fornai L, Glunde K, Heeren RM. An alternative paper based tissue washing method for mass spectrometry imaging: localized washing and fragile tissue analysis. J Am Soc Mass Spectrom. 2011;22(10):1885–90.
57. Angel PM, Spraggins JM, Baldwin HS, Caprioli R. Enhanced sensitivity for high spatial resolution lipid analysis by negative ion mode matrix assisted laser desorption ionization imaging mass spectrometry. Anal Chem. 2012;84(3):1557–64.
58. Hankin JA, Barkley RM, Murphy RC. Sublimation as a method of matrix application for mass spectrometric imaging. J Am Soc Mass Spectrom. 2007;18(9):1646–52.
59. Baluya DL, Garrett TJ, Yost RA. Automated MALDI matrix deposition method with inkjet printing for imaging mass spectrometry. Anal Chem. 2007;79(17):6862–7.
60. Becker L, Carre V, Poutaraud A, Merdinoglu D, Chaimbault P. MALDI mass spectrometry imaging for the simultaneous location of resveratrol, pterostilbene and viniferins on grapevine leaves. Molecules. 2014;19(7):10587–600.
61. Meriaux C, Franck J, Wisztorski M, Salzet M, Fournier I. Liquid ionic matrixes for MALDI mass spectrometry imaging of lipids. J Proteomics. 2010;73(6):1204–18.
62. Anderson DM, Floyd KA, Barnes S, Clark JM, Clark JI, McHaourab H, et al. A method to prevent protein delocalization in imaging mass spectrometry of non-adherent tissues: application to small vertebrate lens imaging. Anal Bioanal Chem. 2015;407(8):2311–20.
63. Fraser PD, Enfissi EM, Goodfellow M, Eguchi T, Bramley PM. Metabolite profiling of plant carotenoids using the matrix-assisted laser desorption ionization time-of-flight mass spectrometry. Plant J. 2007;49(3):552–64.
64. Debois D, Jourdan E, Smargiasso N, Thonart P, De Pauw E, Ongena M. Spatiotemporal monitoring of the antibiome secreted by bacillus biofilms on plant roots using MALDI mass spectrometry imaging. Anal Chem. 2014;86(9):4431–8.
65. Franceschi P, Dong Y, Strupat K, Vrhovsek U, Mattivi F. Combining intensity correlation analysis and MALDI imaging to study the distribution of flavonols and dihydrochalcones in golden delicious apples. J Exp Bot. 2012;63(3):1123–33.
66. Gemperline E, Li L. MALDI-Mass Spectrometric Imaging of Endogenous Metabolites in Biological Systems. eLS, Wiley; 2014. doi:10.1002/9780470015902.a0023207.
67. Horka P, Vrkoslav V, Hanus R, Peckova K, Cvacka J. New MALDI matrices based on lithium salts for the analysis of hydrocarbons and wax esters. J Mass Spectrom. 2014;49(7):628–38.
68. Shroff R, Schramm K, Jeschke V, Nemes P, Vertes A, Gershenzon J, et al. Quantification of plant surface metabolites by matrix-assisted laser desorption-ionization mass spectrometry imaging: glucosinolates on Arabidopsis thaliana leaves. Plant J. 2015;81(6):961–72.

69. Horn PJ, Korte AR, Neogi PB, Love E, Fuchs J, Strupat K, et al. Spatial mapping of lipids at cellular resolution in embryos of cotton. Plant Cell. 2012;24(2):622–36.
70. Cha S, Zhang H, Ilarslan HI, Wurtele ES, Brachova L, Nikolau BJ, et al. Direct profiling and imaging of plant metabolites in intact tissues by using colloidal graphite-assisted laser desorption ionization mass spectrometry. Plant J. 2008;55(2):348–60.
71. Wang X, Han J, Chou A, Yang J, Pan J, Borchers CH. Hydroxyflavones as a new family of matrices for MALDI tissue imaging. Anal Chem. 2013;85(15):7566–73.
72. Yang H, Liu N, Qiu X, Liu S. A New method for analysis of disulfide-containing proteins by matrix-assisted laser desorption ionization (MALDI) mass spectrometry. J Am Soc Mass Spectrom. 2009;20(12):2284–93.
73. Molin L, Seraglia R, Dani FR, Moneti G, Traldi P. The double nature of 1,5-diaminonaphthalene as matrix-assisted laser desorption/ionization matrix: some experimental evidence of the protonation and reduction mechanisms. Rapid Commun Mass Spectrom. 2011;25(20):3091–6.
74. Robichaud G, Barry J, Muddiman D. IR-MALDESI mass spectrometry imaging of biological tissue sections using ice as a matrix. J Am Soc Mass Spectrom. 2014;25(3):319–28.
75. Dufresne M, Thomas A, Breault-Turcot J, Masson J-F, Chaurand P. Silver-assisted laser desorption ionization for high spatial resolution imaging mass spectrometry of olefins from thin tissue sections. Anal Chem. 2013;85(6):3318–24.
76. Jackson SN, Baldwin K, Muller L, Womack VM, Schultz JA, Balaban C, et al. Imaging of lipids in rat heart by MALDI-MS with silver nanoparticles. Anal Bioanal Chem. 2014;406(5):1377–86.
77. Muller L, Kailas A, Jackson SN, Roux A, Barbacci DC, Schultz JA, et al. Lipid imaging within the normal rat kidney using silver nanoparticles by matrix-assisted laser desorption/ionization mass spectrometry. Kidney Int. 2015;88(1):186–92.
78. Wu HP, Yu CJ, Lin CY, Lin YH, Tseng WL. Gold nanoparticles as assisted matrices for the detection of biomolecules in a high-salt solution through laser desorption/ionization mass spectrometry. J Am Soc Mass Spectrom. 2009;20(5):875–82.
79. Jackson SN, Ugarov M, Egan T, Post JD, Langlais D, Albert Schultz J, et al. MALDI-ion mobility-TOFMS imaging of lipids in rat brain tissue. J Mass Spectrom. 2007;42(8):1093–8.
80. Taira S, Sugiura Y, Moritake S, Shimma S, Ichiyanagi Y, Setou M. Nanoparticle-assisted laser desorption/ionization based mass imaging with cellular resolution. Anal Chem. 2008;80(12):4761–6.
81. Schramm T, Hester A, Klinkert I, Both JP, Heeren RM, Brunelle A, et al. imzML-a common data format for the flexible exchange and processing of mass spectrometry imaging data. J Proteomics. 2012;75(16):5106–10.
82. Klinkert I, Chughtai K, Ellis SR, Heeren RMA. Methods for full resolution data exploration and visualization for large 2D and 3D mass spectrometry imaging datasets. Int J Mass Spectrom. 2014;362:40–7.
83. Horn PJ, Chapman KD. Metabolite Imager: customized spatial analysis of metabolite distributions in mass spectrometry imaging. Metabolomics. 2013;10(2):337–48.
84. Paschke C, Leisner A, Hester A, Maass K, Guenther S, Bouschen W, et al. Mirion--a software package for automatic processing of mass spectrometric images. J Am Soc Mass Spectrom. 2013;24(8):1296–306.
85. Robichaud G, Garrard KP, Barry JA, Muddiman DC. MSiReader: an open-source interface to view and analyze high resolving power MS imaging files on Matlab platform. J Am Soc Mass Spectrom. 2013;24(5):718–21.
86. Rübel O, Greiner A, Cholia S, Louie K, Bethel EW, Northen TR, et al. OpenMSI: a high-performance web-based platform for mass spectrometry imaging. Anal Chem. 2013;85(21):10354–61.
87. Bemis KD, Harry A, Eberlin LS, Ferreira C, van de Ven SM, Mallick P, et al. Cardinal: an R package for statistical analysis of mass spectrometry-based imaging experiments. Bioinformatics. 2015;31(14):2418–20.
88. Parry RM, Galhena AS, Gamage CM, Bennett RV, Wang MD, Fernández FM. OmniSpect: an open MATLAB-based tool for visualization and analysis of matrix-assisted laser desorption/

ionization and desorption electrospray ionization mass spectrometry images. J Am Soc Mass Spectrom. 2013;24(4):646–9.
89. Källback P, Nilsson A, Shariatgorji M, Andrén PE. MsIQuant – quantitation software for mass spectrometry imaging enabling fast access, visualization, and analysis of large data sets. Anal Chem. 2016;88(8):4346–53.
90. Takahashi K, Kozuka T, Anegawa A, Nagatani A, Mimura T. Development and application of a high-resolution imaging mass spectrometer for the study of plant tissues. Plant Cell Physiol. 2015;56(7):1329–38.
91. Gamboa-Becerra R, Ramírez-Chávez E, Molina-Torres J, Winkler R. MSI.R scripts reveal volatile and semi-volatile features in low-temperature plasma mass spectrometry imaging (LTP-MSI) of chilli (Capsicum annuum). Anal Bioanal Chem. 2015;407(19):5673–84.
92. Gibb S, Strimmer K. MALDIquant: a versatile R package for the analysis of mass spectrometry data. Bioinformatics. 2012;28(17):2270–1.
93. Alexandrov T. MALDI imaging mass spectrometry: statistical data analysis and current computational challenges. BMC Bioinformatics. 2012;13 Suppl 16:S11.
94. Alexandrov T, Chernyavsky I, Becker M, von Eggeling F, Nikolenko S. Analysis and interpretation of imaging mass spectrometry data by clustering mass-to-charge images according to their spatial similarity. Anal Chem. 2013;85(23):11189–95.
95. Norris JL, Cornett DS, Mobley JA, Andersson M, Seeley EH, Chaurand P, et al. Processing MALDI mass spectra to improve mass spectral direct tissue analysis. Int J Mass Spectrom. 2007;260(2–3):212–21.
96. Franceschi P, Wehrens R. Self-organizing maps: a versatile tool for the automatic analysis of untargeted imaging datasets. Proteomics. 2014;14(7–8):853–61.
97. Fonville JM, Carter CL, Pizarro L, Steven RT, Palmer AD, Griffiths RL, et al. Hyperspectral visualization of mass spectrometry imaging data. Anal Chem. 2013;85(3):1415–23.
98. Wijetunge CD, Saeed I, Halgamuge SK, Boughton B, Roessner U, editors. Unsupervised learning for exploring MALDI imaging mass spectrometry 'omics' data. Information and Automation for Sustainability (ICIAfS), 2014 7th International Conference on; 22–24 Dec. 2014.
99. Andersson M, Groseclose MR, Deutch AY, Caprioli RM. Imaging mass spectrometry of proteins and peptides: 3D volume reconstruction. Nat Methods. 2008;5(1):101–8.
100. Oetjen J, Veselkov K, Watrous J, McKenzie JS, Becker M, Hauberg-Lotte L, et al. Benchmark datasets for 3D MALDI- and DESI-imaging mass spectrometry. Gigascience. 2015;4:20.
101. Weaver EM, Hummon AB, Keithley RB. Chemometric analysis of MALDI mass spectrometric images of three-dimensional cell culture systems. Anal Methods. 2015;7(17):7208–19.
102. Fletcher JS, Lockyer NP, Vickerman JC. Developments in molecular SIMS depth profiling and 3D imaging of biological systems using polyatomic primary ions. Mass Spectrom Rev. 2011;30(1):142–74.
103. Fletcher JS, Vickerman JC, Winograd N. Label free biochemical 2D and 3D imaging using secondary ion mass spectrometry. Curr Opin Chem Biol. 2011;15(5):733–40.
104. McDonnell LA, Rompp A, Balluff B, Heeren RM, Albar JP, Andren PE, et al. Discussion point: reporting guidelines for mass spectrometry imaging. Anal Bioanal Chem. 2015;407(8):2035–45.
105. Creek DJ, Dunn WB, Fiehn O, Griffin JL, Hall RD, Lei Z, et al. Metabolite identification: are you sure? And how do your peers gauge your confidence? Metabolomics. 2014;10(3):350–3.
106. Rompp A, Wang R, Albar JP, Urbani A, Hermjakob H, Spengler B, et al. A public repository for mass spectrometry imaging data. Anal Bioanal Chem. 2015;407(8):2027–33.
107. Anderson DM, Ablonczy Z, Koutalos Y, Spraggins J, Crouch RK, Caprioli RM, et al. High resolution MALDI imaging mass spectrometry of retinal tissue lipids. J Am Soc Mass Spectrom. 2014;25(8):1394–403.
108. Fernandez R, Lage S, Abad-Garcia B, Barcelo-Coblijn G, Teres S, Lopez DH, et al. Analysis of the lipidome of xenografts using MALDI-IMS and UHPLC-ESI-QTOF. J Am Soc Mass Spectrom. 2014;25(7):1237–46.
109. Martin-Lorenzo M, Balluff B, Maroto AS, Carreira RJ, van Zeijl RJ, Gonzalez-Calero L, et al. Molecular anatomy of ascending aorta in atherosclerosis by MS imaging: specific lipid and protein patterns reflect pathology. J Proteomics. 2015;126:245–51.

110. Roux A, Muller L, Jackson SN, Post J, Baldwin K, Hoffer B, et al. Mass spectrometry imaging of rat brain lipid profile changes over time following traumatic brain injury. J Neurosci Methods. 2016. doi:10.1016/j.jneumeth.2016.02.004.
111. Ruh H, Salonikios T, Fuchser J, Schwartz M, Sticht C, Hochheim C, et al. MALDI imaging MS reveals candidate lipid markers of polycystic kidney disease. J Lipid Res. 2013;54(10):2785–94.
112. Uzbekova S, Elis S, Teixeira-Gomes AP, Desmarchais A, Maillard V, Labas V. MALDI mass spectrometry imaging of lipids and gene expression reveals differences in fatty acid metabolism between follicular compartments in porcine ovaries. Biology (Basel). 2015;4(1):216–36.
113. Chatterji B, Dickhut C, Mielke S, Kruger J, Just I, Glage S, et al. MALDI imaging mass spectrometry to investigate endogenous peptides in an animal model of Usher's disease. Proteomics. 2014;14(13–14):1674–87.
114. Gustafsson OJ, Eddes JS, Meding S, McColl SR, Oehler MK, Hoffmann P. Matrix-assisted laser desorption/ionization imaging protocol for in situ characterization of tryptic peptide identity and distribution in formalin-fixed tissue. Rapid Commun Mass Spectrom. 2013;27(6):655–70.
115. Hunt NJ, Phillips L, Waters KA, Machaalani R. Proteomic MALDI-TOF/TOF-IMS examination of peptide expression in the formalin fixed brainstem and changes in sudden infant death syndrome infants. J Proteomics. 2016;138:48–60.
116. Ljungdahl A, Hanrieder J, Bergquist J, Andersson M. Analysis of neuropeptides by MALDI imaging mass spectrometry. Methods Mol Biol. 2013;1023:121–36.
117. Meding S, Martin K, Gustafsson OJ, Eddes JS, Hack S, Oehler MK, et al. Tryptic peptide reference data sets for MALDI imaging mass spectrometry on formalin-fixed ovarian cancer tissues. J Proteome Res. 2013;12(1):308–15.
118. Park KM, Moon JH, Kim KP, Lee SH, Kim MS. Relative quantification in imaging of a peptide on a mouse brain tissue by matrix-assisted laser desorption ionization. Anal Chem. 2014;86(10):5131–5.
119. Sosnowski P, Zera T, Wilenska B, Szczepanska-Sadowska E, Misicka A. Imaging and identification of endogenous peptides from rat pituitary embedded in egg yolk. Rapid Commun Mass Spectrom. 2015;29(4):327–35.
120. Winderbaum LJ, Koch I, Gustafsson OJR, Meding S, Hoffmann P. Feature extraction for proteomics imaging mass spectrometry data. Ann Appl Statistics. 2015;9(4):1973–96.
121. Anderson DM, Van de Plas R, Rose KL, Hill S, Schey KL, Solga AC, et al. 3-D imaging mass spectrometry of protein distributions in mouse Neurofibromatosis 1 (NF1)-associated optic glioma. J Proteomics. 2016. doi:10.1016/j.jprot.2016.02.004.
122. Spraggins JM, Rizzo DG, Moore JL, Noto MJ, Skaar EP, Caprioli RM. Next-generation technologies for spatial proteomics: integrating ultra-high speed MALDI-TOF and high mass resolution MALDI FTICR imaging mass spectrometry for protein analysis. Proteomics. 2016;16(11–12):1678–89.
123. Undheim EA, Hamilton BR, Kurniawan ND, Bowlay G, Cribb BW, Merritt DJ, et al. Production and packaging of a biological arsenal: evolution of centipede venoms under morphological constraint. Proc Natl Acad Sci U S A. 2015;112(13):4026–31.
124. He J, Luo Z, Huang L, He J, Chen Y, Rong X, et al. Ambient mass spectrometry imaging metabolomics method provides novel insights into the action mechanism of drug candidates. Anal Chem. 2015;87(10):5372–9.
125. Wijetunge CD, Saeed I, Boughton BA, Spraggins JM, Caprioli RM, Bacic A, et al. EXIMS: an improved data analysis pipeline based on a new peak picking method for EXploring Imaging Mass Spectrometry data. Bioinformatics. 2015;31(19):3198–206.
126. Zhao YY, Miao H, Cheng XL, Wei F. Lipidomics: Novel insight into the biochemical mechanism of lipid metabolism and dysregulation-associated disease. Chem Biol Interact. 2015;240:220–38.
127. Barry JA, Robichaud G, Bokhart MT, Thompson C, Sykes C, Kashuba AD, et al. Mapping antiretroviral drugs in tissue by IR-MALDESI MSI coupled to the Q Exactive and comparison with LC-MS/MS SRM assay. J Am Soc Mass Spectrom. 2014;25(12):2038–47.

128. Bianga J, Bouslimani A, Bec N, Quenet F, Mounicou S, Szpunar J, et al. Complementarity of MALDI and LA ICP mass spectrometry for platinum anticancer imaging in human tumor. Metallomics. 2014;6(8):1382–6.
129. Huber K, Aichler M, Sun N, Buck A, Li Z, Fernandez IE, et al. A rapid ex vivo tissue model for optimising drug detection and ionisation in MALDI imaging studies. Histochem Cell Biol. 2014;142(4):361–71.
130. Huber K, Feuchtinger A, Borgmann DM, Li Z, Aichler M, Hauck SM, et al. Novel approach of MALDI drug imaging, immunohistochemistry, and digital image analysis for drug distribution studies in tissues. Anal Chem. 2014;86(21):10568–75.
131. Salphati L, Shahidi-Latham S, Quiason C, Barck K, Nishimura M, Alicke B, et al. Distribution of the phosphatidylinositol 3-kinase inhibitors Pictilisib (GDC-0941) and GNE-317 in U87 and GS2 intracranial glioblastoma models-assessment by matrix-assisted laser desorption ionization imaging. Drug Metab Dispos. 2014;42(7):1110–6.
132. Shariatgorji M, Nilsson A, Goodwin RJ, Kallback P, Schintu N, Zhang X, et al. Direct targeted quantitative molecular imaging of neurotransmitters in brain tissue sections. Neuron. 2014;84(4):697–707.
133. Connell JJ, Sugihara Y, Torok S, Dome B, Tovari J, Fehniger TE, et al. Localization of sunitinib in in vivo animal and in vitro experimental models by MALDI mass spectrometry imaging. Anal Bioanal Chem. 2015;407(8):2245–53.
134. Kamata T, Shima N, Sasaki K, Matsuta S, Takei S, Katagi M, et al. Time-course mass spectrometry imaging for depicting drug incorporation into hair. Anal Chem. 2015;87(11):5476–81.
135. Shobo A, Bratkowska D, Baijnath S, Naiker S, Bester LA, Singh SD, et al. Visualization of time-dependent distribution of rifampicin in rat brain using MALDI MSI and quantitative LCMS/MS. Assay Drug Dev Technol. 2015;13(5):277–84.
136. Fujiwara Y, Furuta M, Manabe S, Koga Y, Yasunaga M, Matsumura Y. Imaging mass spectrometry for the precise design of antibody-drug conjugates. Sci Rep. 2016;6:24954.
137. Goodwin RJ, Nilsson A, Mackay CL, Swales JG, Johansson MK, Billger M, et al. Exemplifying the screening power of mass spectrometry imaging over label-based technologies for simultaneous monitoring of drug and metabolite distributions in tissue sections. J Biomol Screen. 2016;21(2):187–93.
138. Hayasaka T. Application of imaging mass spectrometry for drug discovery. Yakugaku Zasshi: J Pharm Soc Japan. 2016;136(2):163–70.
139. Sun N, Fernandez IE, Wei M, Wu Y, Aichler M, Eickelberg O, et al. Pharmacokinetic and pharmacometabolomic study of pirfenidone in normal mouse tissues using high mass resolution MALDI-FTICR-mass spectrometry imaging. Histochem Cell Biol. 2016;145(2):201–11.
140. Yarnold JE, Hamilton BR, Welsh DT, Pool GF, Venter DJ, Carroll AR. High resolution spatial mapping of brominated pyrrole-2-aminoimidazole alkaloids distributions in the marine sponge Stylissa flabellata via MALDI-mass spectrometry imaging. Mol Biosyst. 2012;8(9):2249–59.
141. Louie KB, Bowen BP, McAlhany S, Huang Y, Price JC, Mao JH, et al. Mass spectrometry imaging for in situ kinetic histochemistry. Sci Rep. 2013;3:1656.
142. Seaman C, Flinders B, Eijkel G, Heeren RM, Bricklebank N, Clench MR. "Afterlife experiment": use of MALDI-MS and SIMS imaging for the study of the nitrogen cycle within plants. Anal Chem. 2014;86(20):10071–7.
143. Hanrieder J, Karlsson O, Brittebo EB, Malmberg P, Ewing AG. Probing the lipid chemistry of neurotoxin-induced hippocampal lesions using multimodal imaging mass spectrometry. Surf Interface Anal. 2014;46(S1):375–8.
144. Chughtai S, Chughtai K, Cillero-Pastor B, Kiss A, Agrawal P, MacAleese L, et al. A multimodal mass spectrometry imaging approach for the study of musculoskeletal tissues. Int J Mass Spectrom. 2012;325–327:150–60.

145. Ogrinc Potočnik N, Škrášková K, Flinders B, Pelicon P, Heeren RMA. Gold sputtered fiducial markers for combined secondary ion mass spectrometry and MALDI imaging of tissue samples. Anal Chem. 2014;86(14):6781–5.
146. Amstalden van Hove ER, Blackwell TR, Klinkert I, Eijkel GB, Heeren RMA, Glunde K. Multimodal mass spectrometric imaging of small molecules reveals distinct spatio-molecular signatures in differentially metastatic breast tumor models. Cancer Res. 2010;70(22):9012–21.
147. Soltwisch J, Kettling H, Vens-Cappell S, Wiegelmann M, Muthing J, Dreisewerd K. Mass spectrometry imaging with laser-induced postionization. Science. 2015;348(6231):211–5.